**SETIT 2005**
3rd International Conference: **S**ciences **O**f **E**lectronic,
**T**echnologies **O**f **I**nformation **A**nd **T**elecommunications
March 27-31, 2005 – Tunisia

# Weld defect detection in industrial radiography based digital image processing

N. Nacereddine*, M. Zelmat**, S. S. Belaïfa* and M. Tridi*

**Laboratoire de Traitement de Signal et de l'Image,CSC, Chéraga, Alger*
**nacereddine_naf@hotmail.com**
**s_belaifa@hotmail.com**
**m_tridi@hotmail.com**

***Laboratoire d'Automatique Appliquée,Université de Boumerdes*
**m_zelmat@yahoo.com**

**Abstract:** Industrial radiography is a famous technique for the identification and evaluation of discontinuities, or defects, such as cracks, porosity and foreign inclusions found in welded joints. Although this technique has been well developed, improving both the inspection process and operating time, it does suffer from several drawbacks. The poor quality of radiographic images is due to the physical nature of radiography as well as small size of the defects and their poor orientation relatively to the size and thickness of the evaluated parts.
Digital image processing techniques allow the interpretation of the image to be automated, avoiding the presence of human operators making the inspection system more reliable, reproducible and faster. Perfect knowledge of the geometry of these defects is an important step which is essential to appreciate the quality of the weld.
This paper describes our attempt to develop and implement digital image processing algorithms based on global and local approaches for the purpose of automatic defect detection in radiographic images.
Because of the complex nature of the considered images, and in order that the detected defect region represents the most accurately possible the real defect, the choice of global and local preprocessing and segmentation methods must be appropriated.
**Key words:** Digital image processing, global and local approaches, radiographic film, weld defect.

## 1 Introduction

The industrial radiography is a non-destructive method that uses the penetrating and ionizing inspection radiation to detect internal discontinuities, especially in welded joints (porosity, cracks, lack of penetration, etc.). Mainly used in the petroleum, petrochemical, nuclear and power generation industries especially, for the inspection of welds, the radiography has played an important role in the quality assurance of the piece or component, in conformity with the requirements of the standards, specifications and codes of manufacturing. The reliable detection of defects is one of the most important tasks in non-destructive testing, mainly in the radiographic testing, since the human factor still has a decisive influence on the evaluation of defects on the film. An incorrect classification may disapprove a piece in good conditions or approve a piece with discontinuities exceeding the limit established by the applicable standards (Carvalho & al., 2003).
The expert radiograph has as role to inspect each film in order to detect the presence of possible defects which he must then identify and measure. This work is made particularly delicate because of a low dimension of certain defects (a fissure can have a thickness lower than $200\ \mu m$), a bad contrast and a noised nature of the radiographic film. The expert often works in extreme cases of the visual system and, that is why the subjectivity in the mechanisms of detection and measurement is not negligible.
Perfect knowledge of the geometry of these weld defects is an important step which is essential to appreciate the quality of the weld (Schwartz, 2003).

The radiographic image processing is especially used to improve the image quality, making the analysis process easier, which consists of detecting and classifying defects on the film. In the conventional method, the analysis is done exclusively by the radiograph inspector. The progresses in computer science and the artificial intelligence techniques have allowed the defect classification to be carried out by using pattern recognition tools, which make the process automatic and more reliable, as it is not a subjective analysis (Carvalho & al., 2003). Digital image processing covers the set of the processes of improvement and extraction of qualitative information in digital images, according to the required users and needs, to give us, either new images or particular evaluations.
The purpose of the use of digital image processing techniques is not only to detect and identify the defects automatically (Nacereddine & al.) but also, on the one hand, to offer a better visualization of information and on the other hand to formalize the methods of radiographic expertise in order to make them robust and systematic (Nacereddine, 2004).
In our application, the four first steps (see Figure 1.) of the vision system diagram, dedicated to weld joint radiographic film, will be detailed according to the global and local processing approaches.

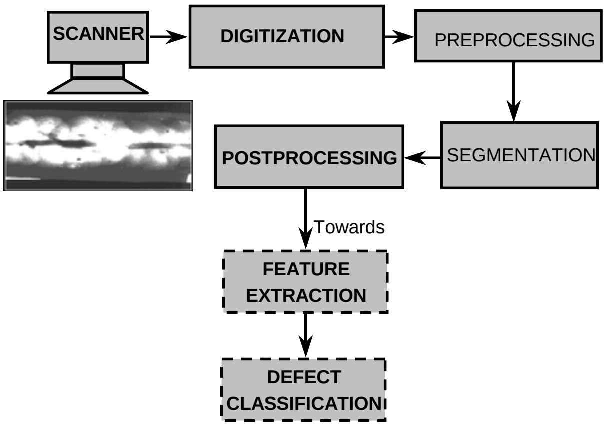


**Figure 1.** *Vision system applied to radiographic films*

Let us examine now each step of image processing: digitization, preprocessing, segmentation and post-processing.

## 2 Digitization

Generally, the radiographic films are very dark and their density is rather large, therefore an ordinary scanner cannot give a sufficient lighting through a radiogram. Of course, specialized scanners adapted to take high quality copies of radiograms exist, but they are expensive. Here, we have used a scanner AGFA Arcus II, (800 dpi, 256 gray levels). The major part of the radiographic films that we have digitized, were extracted from the base the standard films provided by International Institute of Welding (IIW).

After digitization, the principal characteristics of our images are:

- Small contrast between the background and the weld defect regions. These last are characterized by unsharpened and blurred edges.
- Pronounced granularity due to digitization and the type of film used in industrial radiographic testing.
- Presence of background gradient of image characterizing the thickness variation of the irradiated component part.

## 3 Preprocessing

For the reasons evoked in the preceding paragraph, it becomes difficult, if not uncertain to detect, during the radiogram visualization, the presence of the small defects and to determine accurately their sizes. That is why, it is often necessary to start with the preprocessing stage in order to reduce or eliminate the noise enclosing in the film and improve its visibility. This procedure permits to obtain an image which would facilitate later the identification of the weld defects being able to be present in the welded joint. Nevertheless, the first task in image preprocessing is the selection of the region of interest.

### 3.1 Region of interest

The first task, that carryout the radiograph interpreters, is to frame the parts of the image where they suspect the presence of imperfections. For this purpose, the region of interest (ROI) is a reduced zone of the image where the processing will apply. The selection of the ROI saves the operator to make treatments on the useless parts of the image, permitting reduction of the computing time. The second advantage is to save the treatments based on the global approaches to use the irrelevant regions of the image, which can negatively influence the output results. (see Figure 2.).

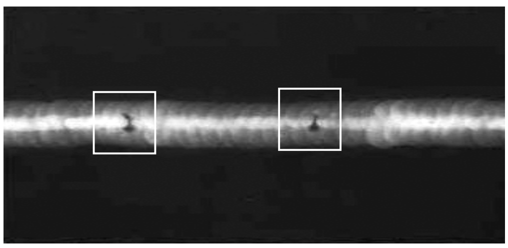

**Figure 2.** *Selection of regions of interest*

In addition, the limitation of the image to a region of interest (ROI) prevents from the detection of false defects outside the weld. We can select only one region per film, as we can have several regions of interests per film.

### 3.2 Noise reduction

Noise in the radiographic image is characterized by its high spatial frequency and its lack of spatial correlation (Kehoe, 1990). Noise reduction is typically carried out by temporal or spatial averaging techniques. Depending on the noise characteristics, other filters such as median filters (impulsive noise), Gaussian smoothening filters (Gaussian white noise), adaptive smoothening filters (signal-dependent white noise) and Kalman filters (signal-dependent colored noise) can also be employed for more complex noise reduction tasks (Zheng &al., 1988).

Radiographic images show substantial variation depending on the testing technique adopted as well as the material being inspected, which makes it difficult to choose a standard filter for noise elimination. Therefore, the right choice is normally made empirically; bearing in mind that use of these filters must not alter the relevant information on those images (Da Silva & al., 2002).

The application of a median type low pass filter is carried out in this paper. This filter performs better than the major averaging filters because it can remove noise from input images with a minimum amount of blurring effect. Its principle can be summarized as follows:

- The gray level values within the specified neighborhood are ordered.
- The current pixel is replaced in the image by the median intensity value of its neighborhood.

The operation of a median filter can be defined as follows:

$$g(x,y) = MEDIAN_{(i,j)\in R(x,y)} f(i,j) \qquad (1)$$

where, *f(x,y)* represents the gray level value of the input image at pixel *(x,y)*, *g(x,y)* represents the gray level value of the smoothed image at pixel *(x,y)*, *R(x,y)* represents a $W \times W$ window centered at pixel *(x,y)* and *MEDIAN* means the median of the gray level values within the specified window.

The main disadvantage of median filtering in a rectangular neighborhood is its damaging of thin lines and sharp corners in the image. This can be avoided if another shape of neighborhood is used.

Figure 3 illustrates the neighborhood used by median filter in our application, where the horizontal and vertical lines are preserved.

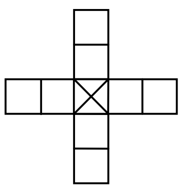

**Figure 3.** *Neighborhood used by median filter*

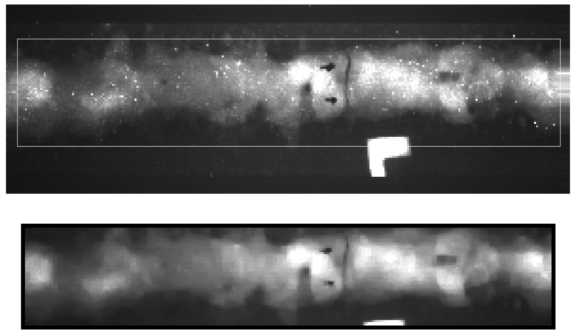

**Figure 4.** *Noise removal by of a median filter*

Figure 4. illustrates the noise removal operation by median filter on radiographic film of welded joint.

### 3.3 Contrast enhancement

The goal of contrast enhancement is to improve the intensity contrast in the input image, highlighting the defect regions whilst leaving the unimportant background regions intact. This enables the defect detection stage to better locate and represent each defect in the image. In our work two techniques are presented for radiographic image contrast enhancement: global contrast enhancement by dynamic stretching (Look Up Table), and local contrast enhancement technique based on the statistical properties of the pixel intensity values taken from a neighborhood around each pixel in the image.

#### 3.3.1 Dynamic stretching

The dynamic stretching is the process that makes the image features of interest stand out more clearly by making optimal use of the gray scale available on the display. Changing the range of values in an image in order to increase differences between features, is accomplished by the redistribution of gray values of the input image histogram so that, the output image histogram occupy a gray level band the largest possible.

A Look-Up Table (LUT) is a transformation of the gray levels of an image with a function that can be linear, logarithmic, or of any type. His aim is to modify the dynamic range of the gray levels in order to improve the visual aspect of the image by expanding original input dynamics to make use of total range or sensitivity of output device. This transformation is best applied to images with Gaussian or near-Gaussian histogram.

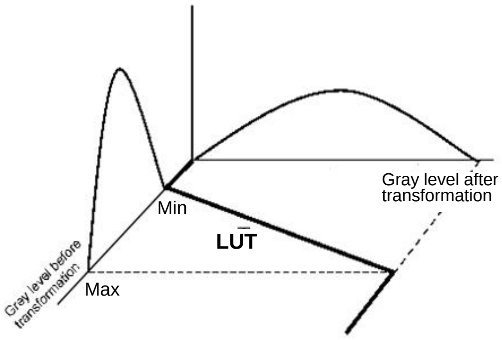


**Figure 5.** *Dynamic stretching principle*

The LUT transformation is given as follows:

$$\begin{gathered} LUT \;:\; Input \;\; image \;\rightarrow\; Output \;\; image \\ f(i,\;j) \rightarrow\; g(i,\;j) \;\;/ \\ g(i,\;j) = \frac{f(i,\;j)\text{ - }Min}{Max\text{ - }Min} \times 255 \end{gathered} \tag{2}$$

Min and Max are, respectively, the minimal and the maximal gray level values in the histogram of the input image.

The below example relate the advantage bearing by LUT transformation in the visibility improvement of radiographic images. The defect in Figure 6.a. is hardly visible to the naked eye. This is due to several factors quoted in § 2. The histogram in Figure 6.b. is condensed at low gray level values because of the dark aspect of the input image. After the application of LUT transformation, the original dynamics is expanded on the total range of gray levels, giving better visibility of the output image (see Figure 6.d).

### 3.3.2 Local contrast enhancement

The method discussed in the previous paragraph is global, in the sense that pixels are modified by a transformation function based on the gray level distribution over an entire image. While this global approach is suitable for overall enhancement, it is often necessary to enhance details over small areas (Gonzalez & al., 1993). For this purpose, the contrast enhancement method developed in this paper is based on the gray level statistical properties of pixels taken in the neighborhood of each pixel in the image.

If we note *f(x, y)* the gray level of the pixel *(x,y)*, then the standard deviation $\sigma(x,y)$ in a $W \times W$ neighborhood centered at *(x,y)* can be computed as :

$$\sigma(x,y) = \left[ \frac{1}{W^2} \sum_{i=-\frac{W-1}{2}}^{\frac{W-1}{2}} \sum_{j=-\frac{W-1}{2}}^{\frac{W-1}{2}} \big( f(x+i,y+j) - \mu(x,y) \big)^2 \right]^{1/2} \tag{3}$$

where $$\mu(x,y) = \frac{1}{W^2} \sum_{i=-\frac{W-1}{2}}^{\frac{W-1}{2}} \sum_{j=-\frac{W-1}{2}}^{\frac{W-1}{2}} f(x+i,y+j) \tag{4}$$

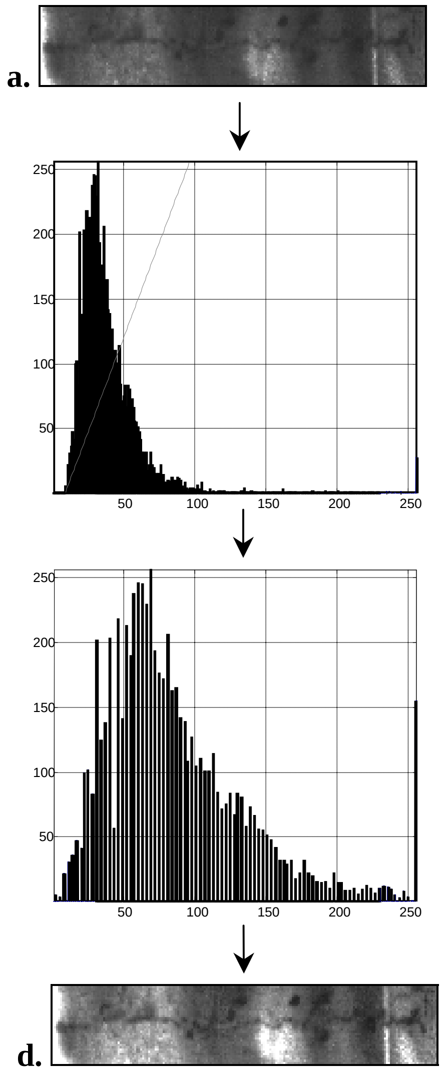


**Figure 6.** *Contrast enhancement by dynamic stretching*

**a.** *Region of interest.* **b.** *Normalized histogram of* ***a.*** *and LUT function (in gray line).* **c.** *Stretched Histogram.* **d.** *Enhanced image.*

$\mu(x,y)$ is gray level mean of *f(x,y)* in the neighborhood $W \times W$. This local contrast enhancement method maps the gray level an input image *f(x,y)* into a new image *g(x,y)* by performing the following transformation at each pixel *(x,y)*.

$$g(x,y) = A(x,y)[f(x,y) - \mu(x,y)] + \mu(x,y) \tag{5}$$

where $$A(x,y) = k\frac{M}{\sigma(x,y)} \qquad 0 < k < 1, \tag{6}$$

*M* is the global mean of *f(x,y)*, and *k* is a constant in the range indicated above. It is important to note that *A*, $\mu$ and $\sigma$ are variable quantities that depend on a predefined neighborhood of *(x,y)*. Application of the local gain factor *A(x,y)* to the difference between *f(x,y)* and the local mean amplifies local variations. Since *A(x,y)* inversely proportional to the standard deviation

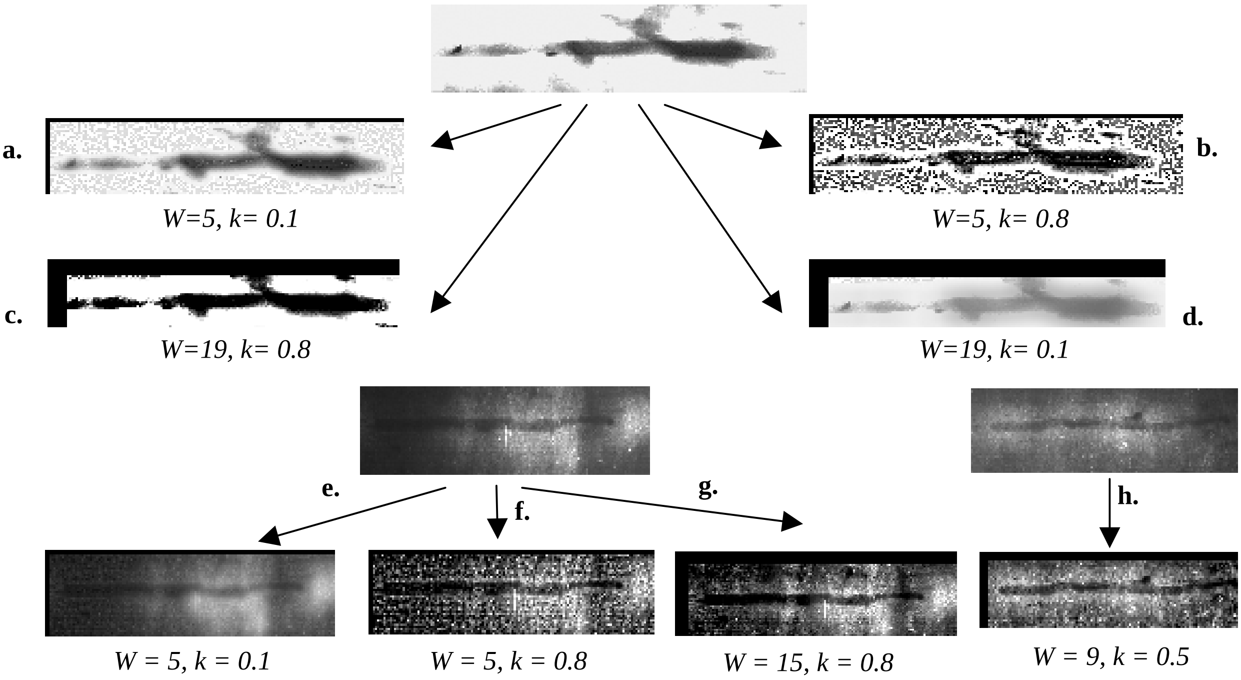


**Figure 7**. *Local method for contrast enhancement*

of the intensity, areas with low contrast receive larger gain. The mean is added back in (5) to restore the average intensity level of the image in the local region.We show in the Figure 7., the results of the contrast enhancement based on this local approach.

According to Figures 7.a, 7.b, 7.c, 7.d, 7.e, 7.f, 7.g and 7.h, the implementation results depend on the amplification factor *k* and the size of the considered neighborhood. A little neighborhood and a big value of amplification factor (near to 1) give a textured aspect of the modified image (Figures 7.b, 7.f). For a little value of *k* (near to 0), the effect of smoothing by neighborhood averaging becomes prevalent (Figures 7.a, 7.d and 7.e). The blurring effect is proportional to the neighborhood size, where it is more pronounced in Figure 7.d compared to Figure 7.a. We obtain better results with amplification factors *k* and neighborhood size rather larges. (see Figures 7.c, 7.g and 7.h). However, it is necessary to take in account the border effect (Figures 7.c and 7.g) when we choose a great neighborhood, that is why, the selected region of interest must be relatively large in order to compensate the masked areas caused by local contrast enhancement algorithm.

## 4 Segmentation

The objective of the segmentation is to describe the significant quantity of information contained in the image by seeking relevant and discriminating visual indices permitting to represent it in more condensed and easily exploitable form. The segmentation constitutes one of the most significant problems in image processing, because the result obtained at the end of this stage strongly governs the final quality of interpretation (Soler & al., 1998).

In digital image processing, we can define the segmentation as the process that subdivides an image in its constituent parts or objects in the form of connected regions having the same properties. These regions can be characterized by:

- their edges, it is the case of the segmentation by edge detection, where we partition an image based on abrupt changes in gray level.
- the pixels which compose them, it concerns then the segmentation in homogeneous regions, of which the purpose is the image segmentation based on intrinsic properties of the region. The principal approaches in this second case are the thresholding, the region-oriented segmentation and the multi-resolution approach.

### 4.1 Thresholding

A very important problem in the design of an image analysis system is to determine the image models and the corresponding segmentation algorithms which are suitable for the image of interest.

The radiographic film images of interest to us contain weld defects placed in background with different intensities. For such images, intensity is a distinguishing feature that can be used to extract the defects from the background. Therefore, a thresholding technique becomes a strong candidate for an efficient radiographic image segmentation.

Thresholding is the process of partitioning pixels in the images into object and background classes based upon the relationship between the gray level value of a pixel and a parameter called the threshold. Because of its efficiency in performance and its simplicity in theory, thresholding techniques have been studied extensively and a large number of thresholding methods have been published (Sezgin & al., 2001). These methods can be divided, among others, into two categories: global methods and local methods. Global methods compute a single threshold value for the entire image, and pixels having a gray level value less than the threshold value are marked belonging to one class, otherwise the other class. Local methods, on the other hand, compute a threshold value for each pixel on the basis of information contained in a local neighborhood of the pixel. The output of a thresholding operation is a binary image.

In the thresholding, i.e. the segmentation of an image into regions of two classes, a threshold *T(x,y)* can be computed for each spatial position *(x,y)*. The segmentation is then done by letting

$$b(x,y)=\begin{cases}0 \quad if \;\; f(x,y)<T(x,y)\\ 1 \quad otherwise\end{cases} \tag{7}$$

where *f* is a gray level input image and *b* is a binary output image.

Based on the properties of the radiographic images, we have implemented three different thresholding algorithms. One of the methods is the Otsu global thresholding and the two others are the Niblack's and Sauvola's local adaptive thresholding.

#### 4.1.1 Global thresholding by Otsu method

Otsu suggested minimizing the weighted sum of within-class variances of the object and background pixels to establish an optimum threshold. Recall that minimization of within-class variances is equivalent to the maximization of between-class variance. This method gives satisfactory results when the numbers of pixels in each class are close to each other.

We give here a summary of this threshold algorithm (Lee & al., 1996). Let the pixels of the image be represented by *V* gray levels *{0,1,2,…,V-1}*. The number of pixels in level *v* is denoted by $n_v$ and thus the total number of pixels is

$$N = n_0 + n_1 + \cdots + n_{V-1} \tag{8}$$

To simplify, the gray level histogram is normalized and regarded as probability distribution function:

$$p_v = n_v / N, \quad p_v \geq 0, \; \sum_{v=0}^{V\text{-}1} p_v = 1 \tag{9}$$

Suppose we divide the pixels into two classes $C_0$ and $C_1$ (background and object) by a threshold value at *k* ; $C_0$ denotes pixels with levels *[0, 1, … , k]* and $C_1$ denotes pixels with levels *[k+1,…, V-1]*. The probabilities of class occurrences $\omega$ and class mean levels $\mu$ for both classes are given by:

$$\begin{cases}\omega_0 = \sum_{v=0}^{k} p_v \\ \omega_1 = 1-\omega_0\end{cases} \quad et \quad \begin{cases}\mu_0 = \dfrac{\mu_k}{\omega_k} \\ \mu_1 = \dfrac{\mu_T-\mu_k}{1-\omega_k}\end{cases} \tag{10}$$

where $\mu_k = \sum_{v=0}^{k} v p_v \,;\; \omega_k = \sum_{v=0}^{k} p_v \,;\; \mu_T = \sum_{v=0}^{V-1} v p_v \,;$ (11)

To measure the thresholding performance, a criterion measure is introduced by Otsu:

$$\eta = \frac{\sigma_B^2}{\sigma_T^2} \tag{12}$$

where

$$\sigma_B^2 = \omega_0(\mu_0-\mu_T)^2 + \omega_1(\mu_1-\mu_T)^2 \tag{13}$$

is the between-class variance, and

$$\sigma_T^2 = \sum_{v=0}^{V-1} (v-\mu_T)^2 p_v \tag{14}$$

is the total variance.

We search for the optimal threshold *k**, which maximize $\eta$, or equivalently maximizing $\sigma_B^2$, since $\sigma_T^2$ is independent of *k*. It only remains to compare the value of all the image pixels to the threshold thus found.

#### 4.1.2 Local thresholding by methods of Niblack and Sauvola

In some radiographic images, the background intensity is variable, and the overlapping between the two classes is therefore large, due to the weld thickness variations, the weak sizes of the defect and the geometrical considerations related to the used radiography technique. In such case, by a global thresholding, we do not obtain the desired results. That is why a local thresholding technique can be employed to overcome the problem. The method of Niblack is fast to implement and easy to apply.

The main idea of Niblack's thresholding method (Niblack, 1986) is to vary the threshold value over the input image, based on the local mean and local standard deviation. The threshold value at pixel *(x,y)* is computed by

$$T(x,y) = \mu(x,y) + k\sigma(x,y) \tag{15}$$

where *k* is an adjustable parameter which depends on the image content, $\mu(x,y)$ *et* $\sigma(x,y)$ are respectively

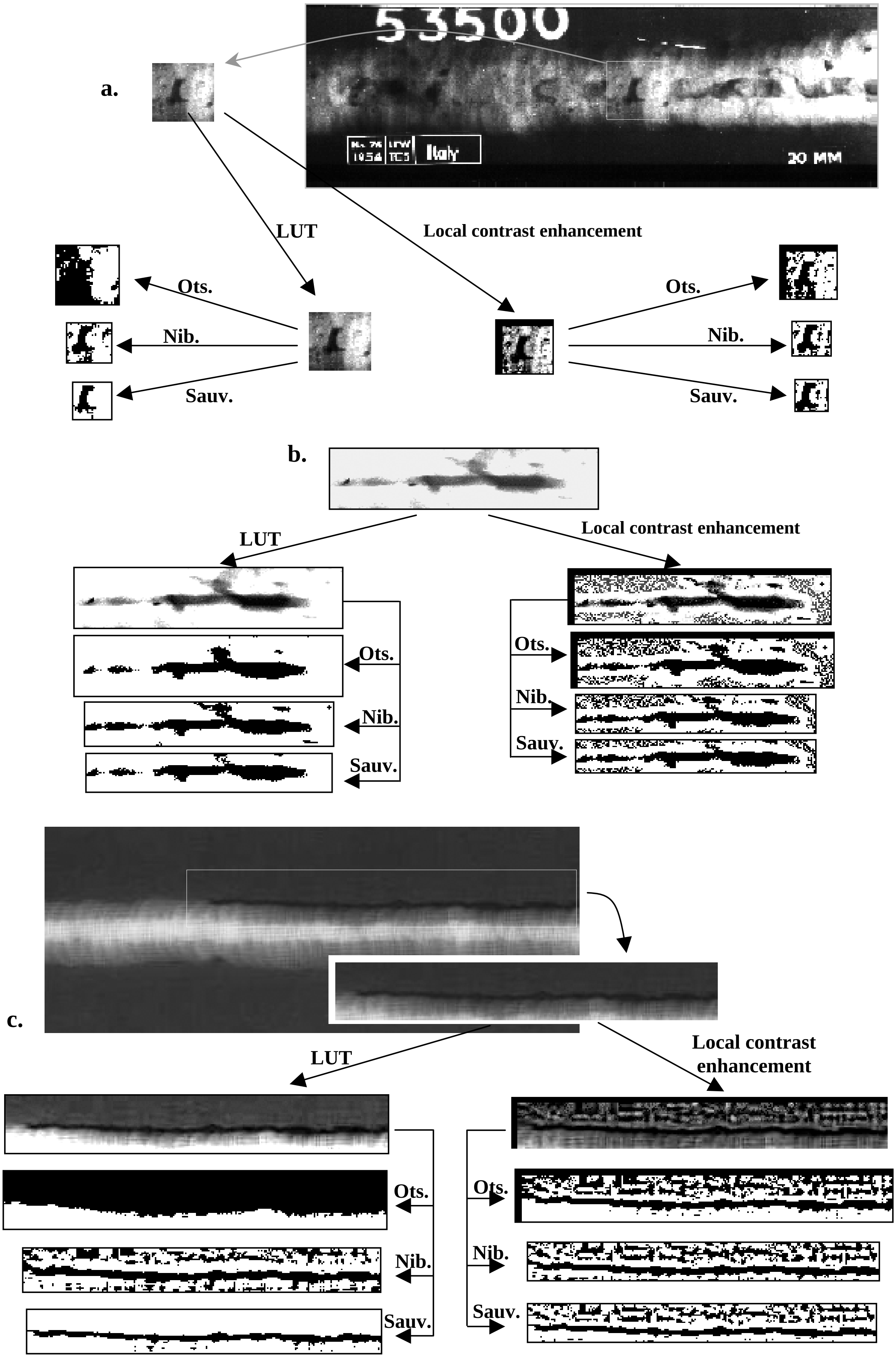


**Figure 8.** *Thresholding results by Otsu, Niblack and Sauvola methods*

the mean and standard deviation of gray level values in a local neighborhood of size $W \times W$ centered at pixel *(x,y)*, and of which the mathematical formulation was already given in the section 3.3.2. The size of the neighborhood must be sufficiently small to preserve the local details but also, it must be enough large to remove the noise.

In (Trier & al., 1995), a neighborhood size of *W=15* and a value of *k=-0.2* were proven satisfactory. In this method, the problems are light textures in the background, which are considered as object with small contrast. To overcome these problems, Sauvola proposed a new improved formula to calculate the threshold:

$$T(x, y) = \mu(x, y)[1 - k\alpha] \tag{16}$$

where $$\alpha = 1 - \frac{\sigma(x, y)}{R} \tag{17}$$

*k :* positive value parameter.
*R :* dynamic range of the variance.

The contribution of the standard deviation becomes adaptive. If we consider for example a dark object on a light background, but with noise, $\mu$ reduces the threshold value in the background regions. The effect of this method is to erase efficiently the noise in the binarized image.

We present in Figures 8.a, 8.b and 8.c, the results of the Otsu, Niblack and Sauvola thresholding methods. We notice that the Otsu method gives good results for well contrasted images i.e. for well separated gray level mode images (see Figure 8.b). This is why; the contrast enhancement proves to be necessary when it can highlight the threshold separating the gray level modes of the image. This method is unsuitable for non uniform background intensity images (Figures 8.a and 8.c). In this case, the methods of Niblack and Sauvola are recommended. This advantage is conferred by the local nature of these tools. Nevertheless, in the Niblack's method, the problem lies in the light textures of the background, which are assimilated to objects with low contrast.

To overcome this problem, the method of Sauvola can be applied. It is noticed that it gives good results on radiographic images, although they are badly contrasted. In fact, in this method, hypothesis on the gray levels of the object and the background are used to eliminate the noise produced by light textures of the background. It should be also known that the performances of these methods are related to choice of the size neighborhood *W* and the parameters *k* and *R*. For the Niblack method, we have taken: *W = 15* and *k = -0.2*. In the Sauvola method, the values of *W = 15*, *k = 0.5* and *R = 128* are selected. This choice was made in an empirical way. All the parameters chosen for these methods must answer the dilemma: robustness / precision. Here, the robustness is the non sensitiveness to noise. On the other hand, the precision is the space definition of the segmented areas.

We illustrate in Figure 9. the role of median filtering in the improvement of thresholding performance. In this example, we notice that the thresholded filtered image by Sauvola method presents less noise compared to that obtained directly without filtering.

## 5 Post-processing and morphological operations

After the thresholding stage, the binary image can contain:

- superfluous information that it is suitable to eliminate,
- or masked information that it is necessary to reveal and this, whatever the employed thresholding method.

The processing based on mathematical morphology makes possible to modify the binary image for this purpose. Mathematical morphology provides an approach to the processing of digital images based on shape. Morphological operations tend to simplify the data image preserving their essential shape characteristics and eliminating irrelevances (Haralick & al., 1987). Dilation and erosion are two basic morphological operations. There are many different ways to define the dilation and the erosion operations for binary images (Haralick & al., 1987) (Pratt, 1991).

Let *b(x,y)* be a binary image where the pixel value is either *1* or *0*, and *H(x,y)* be a structuring element which of the size is $m \times n$.

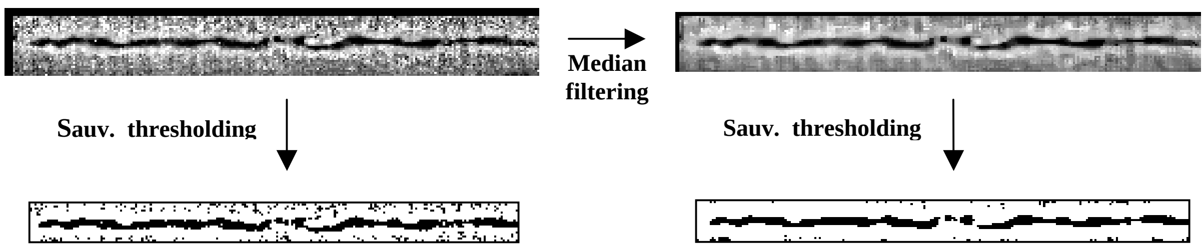


**Figure 9.** *Role of median filtering in the thresholding performance improvement*

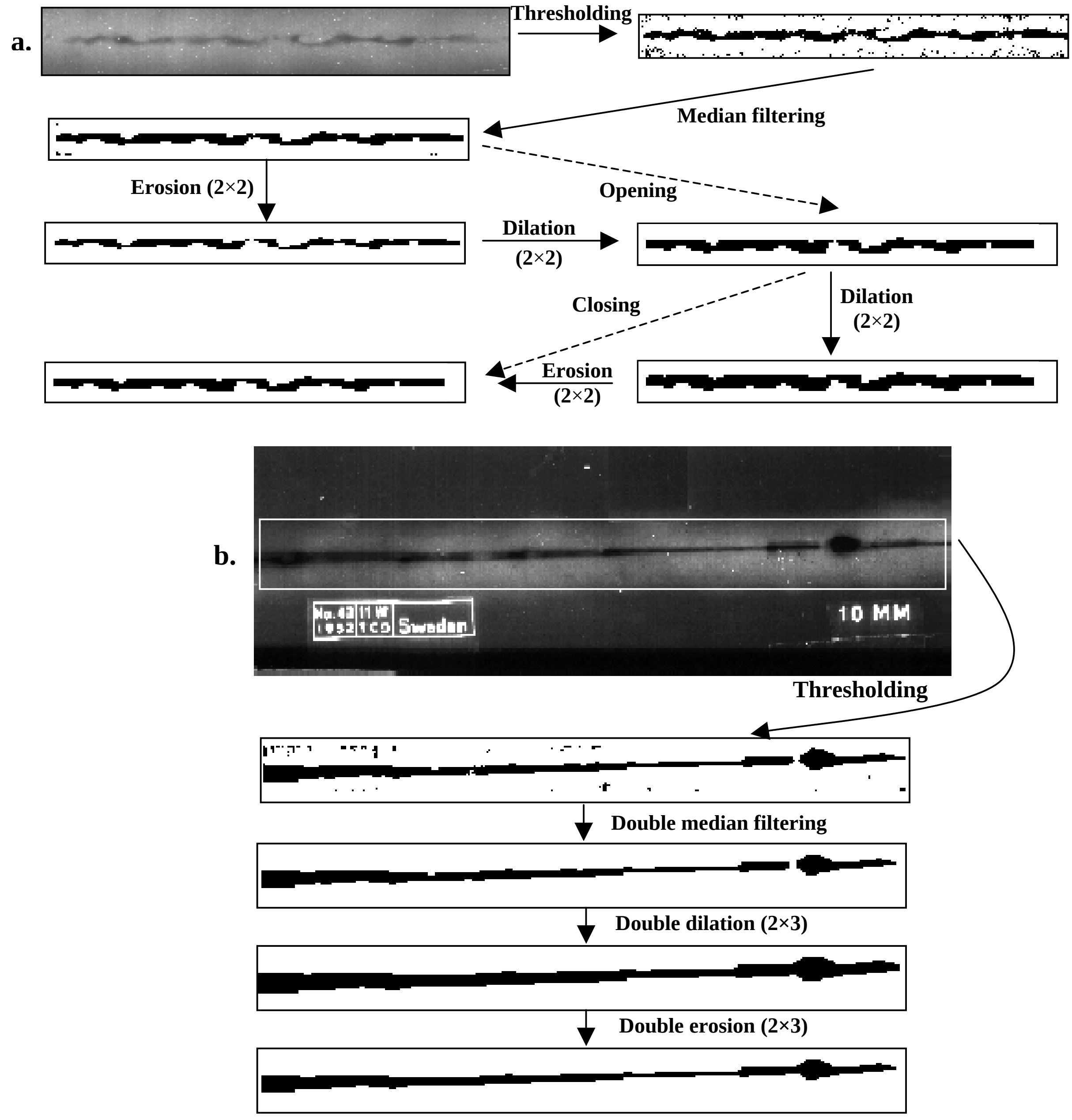


**Figure 10.** *Application of morphological filtering on radiographic binary images*

The definition of the dilation operation $b_{out} = b_{in} \oplus H$ given by Pratt (Pratt, 1991) is

$$b_{out}(x,y) = \bigcup_m \bigcup_n b_{in}(m,n) H(x-m+1, y-n+1) \qquad (18)$$

and that of the erosion operation $b_{out} = b_{in} \Theta H$ is

$$b_{out}(x,y) = \bigcap_m \bigcap_n b_{in}(m,n) \overline{H}(x-m+1, y-n+1) \qquad (19)$$

where $\cup$ and $\cap$ are respectively sequences of binary *OR* and *AND* operations and $\overline{H}$ is the complement of *H* obtained by applying binary *NOT* operations to all the points in *H*.

A structuring element *H* contains a small object, often a disk or another simple shape. The size of the object determines the degree of the dilation or the erosion. Objects in binary images will be thickened after dilation and shrunken after erosion by a disk or a square structuring element. Dilatations and erosions are often used in pairs to obtain opening and closing. The opening of an image *b* by a structuring element *H*, denoted by $b \circ H$, is defined as :

$$b \circ H = (b \,\Theta\, H) \oplus H \qquad (20)$$

The closing of an image *b* by *H*, denoted by $b \bullet H$, is defined as :

$$b \bullet H = (b \oplus H) \,\Theta H \qquad (21)$$

Opening by a disk structuring element smoothes the boundary, breaks narrow parts, and eliminates small objects. Closing by a disk structuring element smoothes the boundary, fills narrow bays, and eliminates small holes.

By referring to morphological operators properties (Haralick, 1987), it thus becomes convenient to apply these operators like their combination in order to eliminate the noise and the small residual spots in the thresholded image. We must consider that at the end of this stage, we obtain only one connected region which represents the more accurately possible, the weld defect and on which we extract various features necessary to the classification stage. The combination of the median filter with the morphological operators of dilation, erosion, opening and closing allows us: to remove the noise, to eliminate the small residual spots and to connect closed regions likely to represent the same weld defect. However, the number of the median filter passes and successive dilations and erosions and the order in which these operators are applied, are related to the nature of the obtained images after thresholding.

In Figure 10.a, one pass of median filter followed by a opening/closing using square structuring element (2×2 of ones) is sufficient to obtain the expected result. On the other hand, in the case of Figure 10.b, it was necessary to apply two passes of median filtering, followed by double dilation and double erosion using a rectangular structuring element (2×3 of ones). This choice is justified by the fact that in this last case, the structuring element must play a double role: eliminate the small irrelevant areas and connect regions which belong a priori to the same region representing the weld defect.

## 6 Conclusion

In the light of the obtained results, we can recommend for the digitized radiographic image processing films the following operations:

- After the selection of the region of interest (ROI) where the defect is likely to be present, we apply a median filter smoothing with one or more passes according to the importance of the noise.
- We apply the dynamic stretching by Look Up Table transformation for uniform background images and the local contrast enhancement method for the images with variable brightness background.
- If the enhanced image histogram is bimodal, it is preferable to apply thresholding by Otsu method. If the defect region after contrast enhancement remains drowned in the background image, it is thus recommended to apply a local thresholding by Niblack or Sauvola methods. Moreover, this latter can be implemented to images with noised background lowly contrasted.
- For the extraction of the defect region, we can apply in an interactive way the median filter and/or the morphological operators in order to eliminate the small residual spots and the small holes and in order to connect the closely regions.

## References

A. A. de Carvalho & al. Evaluation of the relevant features of welding defects in radiographic inspection. *Materials Research*, vol. 6, n° 3, 427-432, 2003.

R.R. Da Silva & al. Contribution to the development of a radiographic inspection automated system. *8^e ECNDT*, Barcelone, June 2002.

R.C. Gonzalez, R.E. Woods. *Digital Image Processing.* Addison Wesley Publishing Company, 1993.

R.M. Haralick, S.R. Sternberg, X. Zhuang. Image analysis using mathematical morphology. *IEEE Trans. on PAMI*, vol.9/4, pp.532-550, 1987.

A. Kehoe. The detection and evaluation of defects in industrial images. Ph.D. Thesis, University of Surrey, 1990.

A.K. Lee & S.P. Wong. A mathematical morphological approach for segmenting heavily noise-corrupted images. *Pattern Recognition*, vol. 29, 1996.

N. Nacereddine & al. Weld defect extraction and identification in radiograms based neural networks. *IASTED International Conference (SPPRA)*, Grèce, Juin 2002.

N. Nacereddine. Mise au point d'une méthode automatisée de detection et classification des défauts de soudures en radiographie industrielle. Master thesis, Université de Boumerdes, Juillet 2004.

W. Niblack. *Introduction to digital image processing.* Prentice Hall, 1986.

W. K. Pratt. *Digital image processing.* Wiley Interscience, 2nd edition, 1991

Ch. Schwartz. Automatic Evaluation of Welded Joints Using Image Processing on Radiographs. *Conference Proceedings American Institute of Physics,* vol 657(1) pp. 689-694. March 27, 2003.

M. Sezgin, B. Sankur. Comparison of thresholding methods for non-destructive testing applications. *IEEE Conference on Image Processing*, Grèce. Oct. 2001.

L. Soler, G. Malandrin, H. Delinguette. Segmentation automatique: Application aux angioscanners 3D. *Revue de Traitement de Signal*, vol. 15, 1998.

O.D. Trier & A.K. Jain. Goal-directed evaluation of binarization methods. *IEEE Trans. Pattern Analysis and Machine Intelligence*, vol.17, pp. 1191-1201, 1995.

Y. Zheng, J.P. Basart. Image analysis, feature extraction and various applied enhancement methods for NDE X-Ray images. *Review of Progress in QNDE*, vol. 7, pp. 813-820, 1988.